Faculty of Electrical Engineering
Universiti Teknologi Malaysia

VOL. 11, NO. 1, 2009, 1-7

ELEKTRIKA
http://fke.utm.my/elektrika

Active Control of High-Speed Railway Vehicles

Hazlina Selamat [1*] and **Mohd Anwar Zawawi** [2]

[1]Faculty of Electrical Engineering, Universiti Teknologi Malaysia, 81310 UTM Skudai, Johor, Malaysia.
[2]Faculty of Electrical & Electronics Engineering, Universiti Malaysia Pahang, Lebuhraya Tun Razak, 26300 Kuantan, Pahang, Malaysia.

[*]Corresponding author: hazlina@fke.utm.my, Tel: 607-5535324, Fax: 607-5566262.

Abstract: This paper presents the active suspension control for bogie-based and two-axle railway vehicles. A bogie-based and a two-axle railway vehicle with solid-axle wheelsets, and a two-axle vehicle with independently rotating wheelsets (IRWs) are considered. The curving performance of each vehicle is presented and compared. The findings in this work show that the two-axle vehicle performs better during curving than the bogie-based vehicle especially when minimum wheelset lateral displacement (for reduced wear and tear of the wheelset) and control effort are of the main concern. It also has the advantage of lighter and simpler configuration. The simulation results also show that the IRW provide better curving performance than the solid-axle wheelset.

Keywords: Active suspension control, independently-rotating wheelset, railway vehicle, two-axle bogie-based.

1. INTRODUCTION

Solid axle wheelsets have been widely used in most railway vehicles. It consists of two wheels that are rigidly connected to a common axle. This arrangement, together with the conical (or profiled) shape of the wheel treads offers the wheelset a self-steering capability when it travels on a track. However, it also causes an unconstrained wheelset to exhibit sinusoidal motion of growing amplitude if disturbed laterally [1]. This is the main reason of the wheelset's, and hence the rail vehicle's instability [2]. Stabilisation of the wheelset is therefore necessary when used on rail vehicles especially if the vehicle is designed to run at high speeds.

In general, a railway vehicle consists of a set of primary and secondary suspension systems. The primary suspension deals with the running stability of the vehicle whereas the secondary suspension transmits the low frequency intended movements so the vehicle follows the track and at the same time isolates the higher frequency vertical irregularities to provide a good ride quality. A *passive suspension* system uses only mechanical springs and dampers, arranged in certain configurations, to transmit curving forces and to stabilise the wheelsets. However, it is difficult to achieve good ride quality, vehicle stability and wheelset curving performance simultaneously when only the passive suspension system is used [3]. That is why the application of active control involving the use of sensors, actuators and electronic controllers to a railway suspension system resulting in an *active suspension* system are being experimented with, as it can provide promising solutions to many suspension design problems.

One of the approaches to overcome the problem inherent in the solid-axle wheelset is by replacing it with the independently-rotating wheelset (IRW). The IRW is a modified version of the basic wheelset where the wheels are allowed to rotate independently on the axle [4]. Despite its ability to increase the critical speed of railway vehicles with proper suspension design [5], natural curving ability is lost due to the disappearance of connection between the two wheels on the wheelset. This increases the wheelset's proneness to derailment and so it requires some sort of steering action to keep the wheelset properly aligned on curves. Moreover, a study in [6] has reported that IRW exhibits quasi-kinematic oscillation, in contrast with the belief that its use removes the instability of the solid-axle wheelset. However, its instability is much easier to overcome than with the solid-axle wheelset, and control action is needed primarily to steer the wheelset.

Figure 1 shows the active suspension arrangement for the two types of railway wheelset used in the work presented in this paper. The wheelsets are controlled using an established technique of active yaw damping in which a rotary actuator replaces the longitudinal springs (springs that is normally attached in longitudinal direction to stabilize the wheelset) to provide yaw torque.

This paper addresses the application of active control in the primary suspension of three types of railway vehicles system: (1) A bogie-based vehicle with solid-axle wheelsets, (2) a two--axle vehicle with solid-axle wheelsets and (3) a two-axle vehicle with IRWs.

2. RAILWAY VEHICLE MODELS

The plan view diagram of a conventional bogie-based vehicle with passive suspension system is shown in Figure 2. The active primary suspension system is obtained by adding the rotary actuator on each of the wheelsets, as shown in Figure 1(a). Since the primary suspension design involves mainly lateral analysis of the system, only the plan view model is considered. The primary suspension consists of all the springs and dampers that connect the wheelset and the bogie whereas

the secondary suspension is made up of those connecting the bogie and the vehicle body. The dynamic equations of the system consists of 28 states, which describe the displacement and velocity in lateral and yaw directions for all the four wheelsets, the two bogies and the vehicle body.

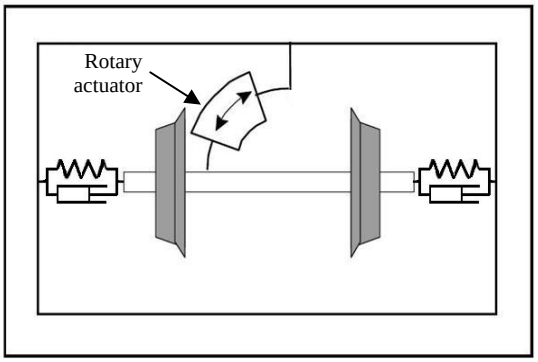

(a) Actively-stabilised solid-axle wheelset

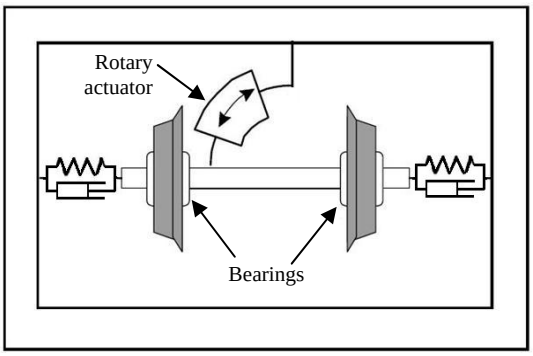

(b) Actively-stabilised IRW

Figure 1. Active suspension system for railway wheelset.

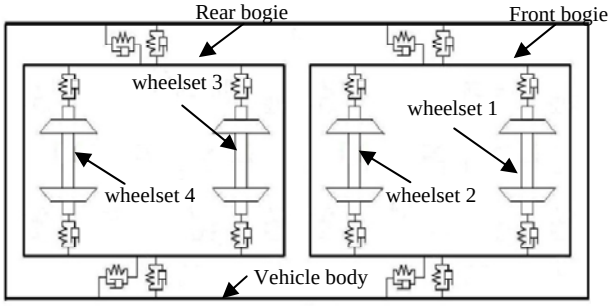

Figure 2. Plan view diagram of a bogie-based railway vehicle

The two-axle railway vehicle system with solid-axle wheelsets features a vehicle without any bogie. The vehicle body is connected directly to the wheelsets via the primary and secondary suspensions, hence reducing its weight and complexity. Its state space consists of only 12 states, which represent the lateral displacement, yaw angle, lateral velocity and yaw velocity for each leading and trailing wheelsets and vehicle body. The equations of motion of the two-axle vehicle with IRW is similar to the two-axle railway vehicle system with solid-axle wheelsets, but two more additional states are required to represent relative rotating velocities between two wheels at front and rear wheelsets. The state equation for the railway vehicle system can be written as

$$\dot{x} = Ax + Bu + Gw \tag{1}$$

where x is the state, u is the control torque and w is the deterministic track input. A, B and G are the system, input and disturbance matrices respectively. w for the bogie-based vehicle with solid-axle wheelsets, two-axle vehicle with solid-axle wheelsets and two-axle vehicle with IRWs are:

$$\begin{bmatrix} 1/R_1 & \theta_{c1} & 1/R_2 & \theta_{c2} & 1/R_3 & \theta_{c3} & 1/R_4 & \theta_{c4} \end{bmatrix}^T,$$
$$\begin{bmatrix} 1/R_1 & \theta_{c1} & 1/R_2 & \theta_{c2} \end{bmatrix}^T,$$
$$\begin{bmatrix} 1/R_1 & \theta_{c1} & 1/R_2 & \theta_{c2} \end{bmatrix}^T$$

The states for all the three vehicle models are given in Table 1.

Table 1: States for three types of vehicle

Vehicle type	**State, x**
Bogie-based vehicle with solid-axle wheelsets	$[\dot{y}_{w1} \quad y_{w1} \quad \dot{\theta}_{w1} \quad \theta_{w1} \quad \dot{y}_{w2} \quad y_{w2} \quad \dot{\theta}_{w2} \quad \dot{\theta}_{w2} \quad \dot{y}_{b1} \quad y_{b1} \quad \dot{\theta}_{b1} \quad \theta_{b1} \quad \dot{y}_{w3} \quad y_{w3} \quad \dot{\theta}_{w3} \quad \theta_{w3} \quad \dot{y}_{w4} \quad y_{w4} \quad \dot{\theta}_{w4} \quad \dot{\theta}_{w4} \quad \dot{y}_{b2} \quad y_{b2} \quad \dot{\theta}_{b2} \quad \theta_{b2} \quad \dot{y}_v \quad y_v \quad \dot{\theta}_v \quad \theta_v]$
Two-axle vehicle with solid-axle wheelsets	$[\dot{y}_{w1} \quad y_{w1} \quad \dot{\theta}_{w1} \quad \theta_{w1} \quad \dot{y}_{w2} \quad y_{w2} \quad \dot{\theta}_{w2} \quad \dot{\theta}_{w2} \quad \dot{y}_v \quad y_v \quad \dot{\theta}_v \quad \theta_v]$
Two-axle vehicle with IRWs	$[\dot{y}_{w1} \quad y_{w1} \quad \dot{\theta}_{w1} \quad \theta_{w1} \quad \dot{y}_{w2} \quad y_{w2} \quad \dot{\theta}_{w2} \quad \dot{\theta}_{w2} \quad \dot{y}_v \quad y_v \quad \dot{\theta}_v \quad \theta_v \quad \phi_{w1} \quad \phi_{w2}]$

A, B and G matrices for the two-axle vehicle [7] are as below. The symbols and parameters used are as given in the Appendix.

$$A=\begin{bmatrix} a_{1,2} & a_{1,2} & 0 & a_{1,4} & 0 & 0 & 0 & 0 & a_{1,9} & a_{1,10} & a_{1,11} & a_{1,12} \\ 1 & 0 & 0 & 0 & 0 & 0 & 0 & 0 & 0 & 0 & 0 & 0 \\ 0 & a_{3,2} & a_{3,3} & 0 & 0 & 0 & 0 & 0 & 0 & 0 & 0 & 0 \\ 0 & 0 & 1 & 0 & 0 & 0 & 0 & 0 & 0 & 0 & 0 & 0 \\ 0 & 0 & 0 & 0 & a_{5,5} & a_{5,6} & 0 & a_{5,8} & a_{5,9} & a_{5,10} & a_{5,11} & a_{5,12} \\ 0 & 0 & 0 & 0 & 1 & 0 & 0 & 0 & 0 & 0 & 0 & 0 \\ 0 & 0 & 0 & 0 & 0 & a_{7,6} & a_{7,7} & 0 & 0 & 0 & 0 & 0 \\ 0 & 0 & 0 & 0 & 0 & 0 & 1 & 0 & 0 & 0 & 0 & 0 \\ a_{9,1} & a_{9,2} & 0 & 0 & a_{9,5} & a_{9,6} & 0 & 0 & a_{9,9} & a_{9,10} & 0 & 0 \\ 0 & 0 & 0 & 0 & 0 & 0 & 0 & 0 & 1 & 0 & 0 & 0 \\ a_{11,1} & a_{11,2} & 0 & 0 & a_{11,5} & a_{11,6} & 0 & 0 & 0 & 0 & a_{11,11} & a_{11,12} \\ 0 & 0 & 0 & 0 & 0 & 0 & 0 & 0 & 0 & 0 & 1 & 0 \end{bmatrix}$$

$$B=\begin{bmatrix} 0 & 0 \\ 0 & 0 \\ 1/I_w & 0 \\ 0 & 0 \\ 0 & 0 \\ 0 & 0 \\ 0 & 1/I_w \\ 0 & 0 \\ 0 & 0 \\ 0 & 0 \\ -1/I_v & -1/I_v \\ 0 & 0 \end{bmatrix}, G=\begin{bmatrix} V^2 & -g & 0 & 0 \\ 0 & 0 & 0 & 0 \\ 2f_{11}l^2/I_w & 0 & 0 & 0 \\ 0 & 0 & 0 & 0 \\ 0 & 0 & V^2 & -g \\ 0 & 0 & 0 & 0 \\ 0 & 0 & 2f_{11}l^2/I_w & 0 \\ 0 & 0 & 0 & 0 \\ V^2/2 & -g/2 & V^2/2 & -g/2 \\ 0 & 0 & 0 & 0 \\ 0 & 0 & 0 & 0 \\ 0 & 0 & 0 & 0 \end{bmatrix}$$

Table 2: Output matrix for three types of vehicle for lateral displacement at wheelset 1

Vehicle type	Output matrix, C
Bogie-based vehicle with solid-axle wheelsets	$C=[0\ 1\ 0\ 0\ 0\ 0\ 0\ 0\ 0\ 0\ 0\ \cdots\ 0\ 0\ 0]$
Two-axle vehicle with solid-axle wheelsets	$C=[0\ 1\ 0\ 0\ 0\ 0\ 0\ 0\ 0\ 0]$
Two-axle vehicle with IRWs	$C=[0\ 1\ 0\ 0\ 0\ 0\ 0\ 0\ 0\ 0\ 0\ 0]$

For the bogie based vehicle, its system, input and disturbance matrices (A_b, B_b, G_b) can be extended from the two-axle vehicle's matrix A above, where

$$A_b=\begin{bmatrix} A_{11} & A_{12} & A_{13} \\ A_{21} & A_{22} & A_{23} \\ A_{31} & A_{32} & A_{33} \end{bmatrix}$$

with A_{11}=A_{22}= matrix A for two axle vehicle, A_{12}=A_{21} = zeros (12,12), A_{13}=A_{23}= zeros (12,4).

$$A_{31}=\begin{bmatrix} & C_s/m_v & K_s/m_v & \\ 0_{4\times8} & 0 & 0 & 0_{4\times2} \\ & C_s l_v/m_v & K_s l_v/m_v & \\ & 0 & 0 & \end{bmatrix}$$

$$A_{32}=\begin{bmatrix} & C_s/m_v & K_s/m_v & \\ 0_{4\times8} & 0 & 0 & 0_{4\times2} \\ & -C_s l_v/m_v & -K_s l_v/m_v & \\ & 0 & 0 & \end{bmatrix}$$

$$A_{33}=\begin{bmatrix} -2C_s/m_v & -2K_s/m_v & 0 & 0 \\ 1 & 0 & 0 & 0 \\ 0 & 0 & -2C_s l_v^2/I_v & -2K_s l_v^2/I_v \\ 0 & 0 & 1 & 0 \end{bmatrix}$$

where $0_{n\ x\ m}$ is a (n x m) zero matrix.

For the input matrix,

$$B_b=\begin{bmatrix} B_{11} & B_{12} \\ B_{21} & B_{22} \\ B_{31} & B_{32} \end{bmatrix}$$

where, B_{12} = B_{21} = zeros (12,2), B_{31} = B_{32}= zeros (4,2), and

$$B_{11}=B_{22}=\begin{bmatrix} 0 & 0 & 1/I_w & 0 & 0 & 0 & 0 & 0 & 0 & 0 & -1/I_b & 0 \\ 0 & 0 & 0 & 0 & 0 & 0 & 1/I_w & 0 & 0 & 0 & -1/I_b & 0 \end{bmatrix}^T$$

The disturbance matrix,

$$G_b=\begin{bmatrix} G_{11} & G_{12} \\ G_{21} & G_{22} \\ G_{31} & G_{32} \end{bmatrix}$$

where G_{11}=G_{22} = matrix G for two axle vehicle, G_{12}= G_{21}= zeros (12,4), G_{31}= G_{32}= zeros (4,4).

It is clear from the state space models above that the railway vehicle is a high-order and complex MIMO system and control of the system is not easy. Moreover, the curving performance of the vehicle is very much affected by the cant angle and the curve radius of the track.

Based on the United States standard rail gauge value of 1435 mm [8] and for safety purposes, the maximum allowable cant deficiency is seven inches or 177.8 mm. Thus, in this paper, the cant angle is selected at 7^o with a curve radius of 1500 m. This will give the superelevation that is equal to 176.2 mm, which is within the permitted limits. Also, there were transition periods of 1 s before and after the curve, during which the curve radius and the amount of cant progressively increased or decreased when the vehicle entered (at t = 1 s) and left (at t = 7 s) the curve. These transitions are a deliberate feature of railway track design to ensure the passengers' comfort.

3. CONTROLLER DESIGN

Active control of railway vehicle's active suspension system is as shown in Figure 3 below [9]. The objective of the controller is to minimize the wheelset's lateral deflection and its yaw angle. Linear quadratic regulator (LQR) is selected as the controller. The setting of the LQR controller is found by using mathematical algorithm that minimizes the cost function while weighting factors determined by the designer. When designing the LQR optimal controller, the system is assumed to be linear and has the following state and output equations:

$$\dot{x} = Ax + Bu \tag{2}$$

$$y = Cx \tag{3}$$

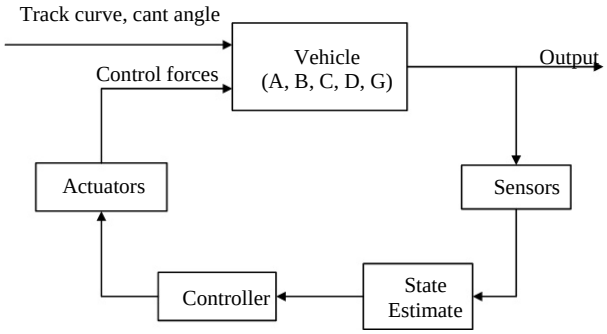

Figure 3. Control structure

The control law is chosen such that it minimizes the cost function below [6]:

$$J = \int \left(y^T(t) \cdot Q \cdot y(t) + u^T(t) \cdot R \cdot u(t) \right) dt \tag{4}$$

where y are as given in Table 3.

Table 3: States to be controlled, y

Vehicle type	States feedback, y
Bogie-based vehicle with solid-axle wheelsets	$[y_{w1} \quad \theta_{w1} \quad y_{w2} \quad \theta_{w2} \quad y_{w3} \quad \theta_{w3} \quad y_{w4} \quad \theta_{w4}]^T$
Two-axle vehicle with solid-axle wheelsets	$[y_{w1} \quad \theta_{w1} \quad y_{w2} \quad \theta_{w2}]^T$
Two-axle vehicle with IRWs	$[y_{w1} \quad \theta_{w1} \quad y_{w2} \quad \theta_{w2}]^T$

The weighting matrices (Q and R) selected for the minimization of LQR cost function given in Equation 4 are given in Table 4. The weighting matrices Q and R have been chosen such that they result in the contribution of each controlled state being roughly equal and satisfactory overall control performance. Notice that the value of R was rather small implying that control effort minimisation is minimal. This is because the amount of the lateral displacement of the wheelset that can be allowed is extremely small, which is approximately 7 mm before flange contact occurs and so the amount of control effort required is large. As will be seen in Section 4 of this paper (in Figure 7), this has resulted in the amount of control torque produced being less than 2.5kNm, which is acceptable.

Table 4: LQR weighting matrices value

Vehicle type	Q	R
Bogie-based vehicle with solid-axle wheelsets	*diag* (0.5,0.01, 0.5,0.01,0.5,0.01, 0.5,0.01)	*diag* (10^{-12},10^{-12}, 10^{-12},10^{-12}]
Two-axle vehicle with solid-axle wheelsets	*diag* (0.1,0.01, 0.1,0.01)	*diag* (10^{-12},10^{-12})
Two-axle vehicle with IRWs	*diag* (100,10, 100,10)	*diag* (10^{-12},10^{-12})

4. RESULTS AND DISCUSSIONS

The curving performance of each of the vehicles considered in the study, using the linear quadratic regulator designed in Section 3, is looked at in terms of the wheelset lateral displacement, wheelset yaw angle, vehicle body acceleration and control effort. Figures 4 to 7 compare the curving performance of the bogie-based and the two-axle railway vehicle.

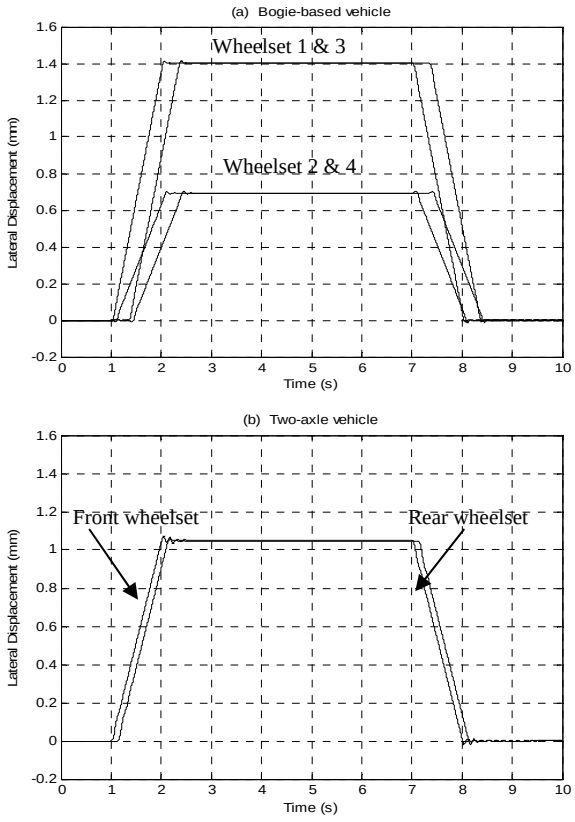

Figure 4. Response of the wheelset lateral displacements (mm)

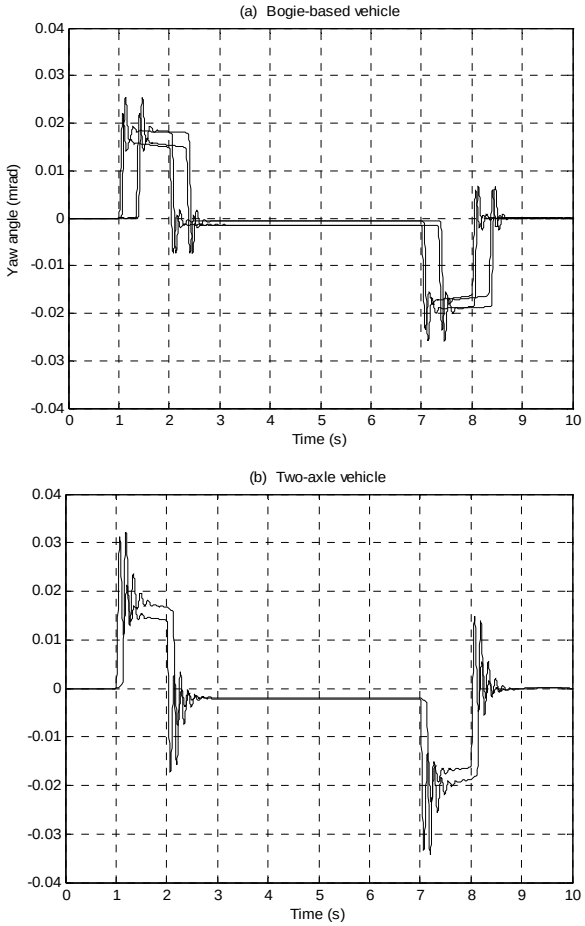

Figure 5. Response of the wheelset yaw angle (mrad)

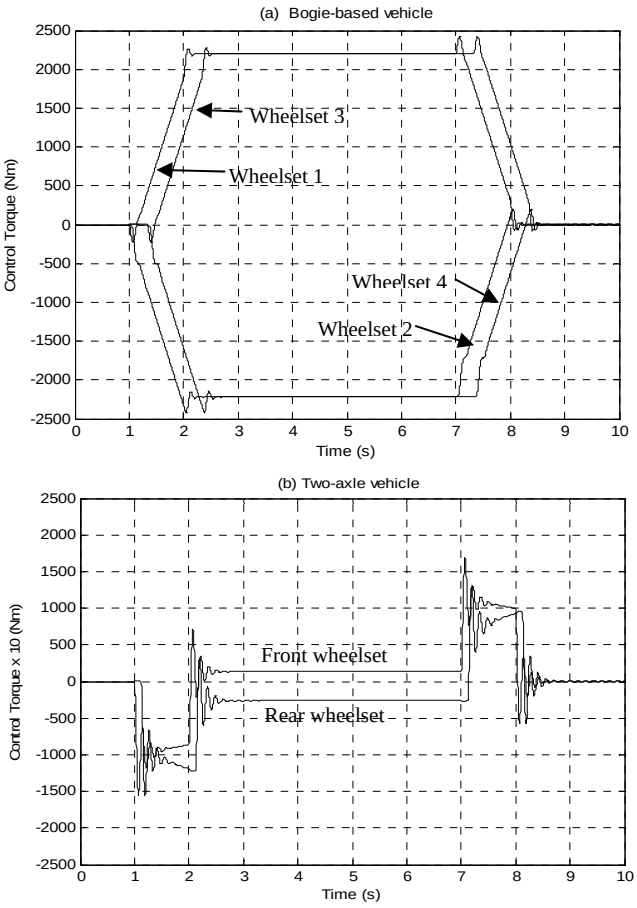

Figure 7. Control Torque (Nm)

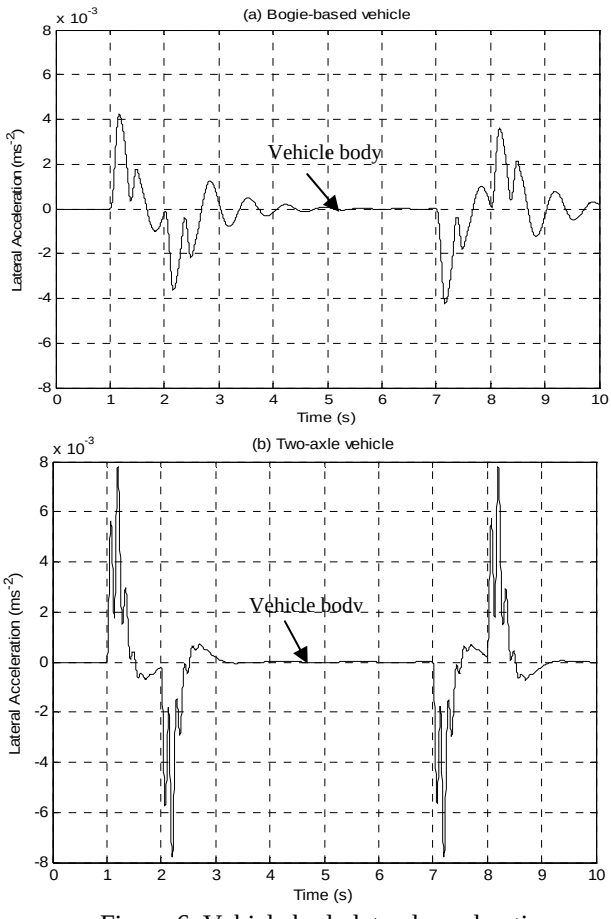

Figure 6. Vehicle body lateral acceleration

It can be seen clearly from Figure 4 that the wheelset lateral displacement of the two-axle vehicle (two plots represent the front and rear wheelsets) is better than the bogie-based vehicle (four plots represent the front and rear wheelsets at each bogie), where unlike the bogie-based vehicle; all the wheelsets of the two-axle vehicle are nicely aligned as they travel round the curve. The yaw angles of both vehicles are very similar (Figure 5). Figure 6 shows that the body of the two axle vehicle settles more quickly as it enters the steady curve whereas the body of the bogie-based vehicle vibrates longer although with smaller amplitude of acceleration. Moreover, the amount of control effort required by the two-axle vehicle is less than one-tenth that of the bogie-based vehicle and is mainly during the curve transitions only (Figure 7).

When comparing the two-axle vehicle with solid-axle wheelsets and IRW, Figure 8 shows that the lateral displacement for two-axle vehicle with IRW is only about 0.3 mm during steady curve - much smaller than that of the vehicle with solid-axle wheelsets, which produced the lateral displacement of about 1.1 mm. The yaw angle is 0.005 mrad, significantly smaller than 0.04 mrad for the one with solid-axle. Besides that, the maximum body acceleration for the two-axle vehicle with IRW is only about 0.002 ms^{-2}, which is a quarter of its solid-axle counterpart. The control torque required for this arrangement is also very small - at 25 Nm (see Figure 8(d)) compared to 2500 Nm for bogie based vehicle with

solid-axle wheelsets as shown in Figure 7(a), and 200 Nm for two-axle vehicle (Figure 7(b)), also with solid-axle wheelsets.

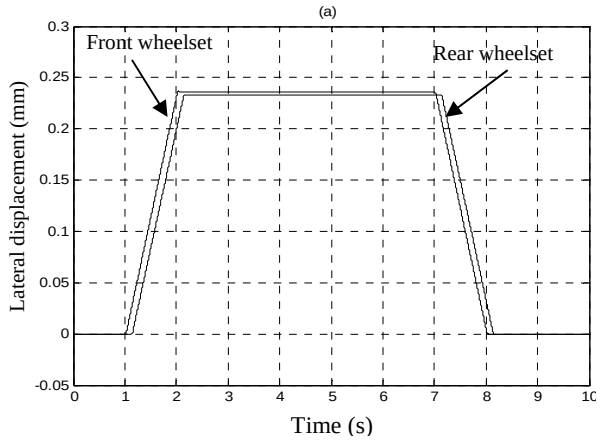

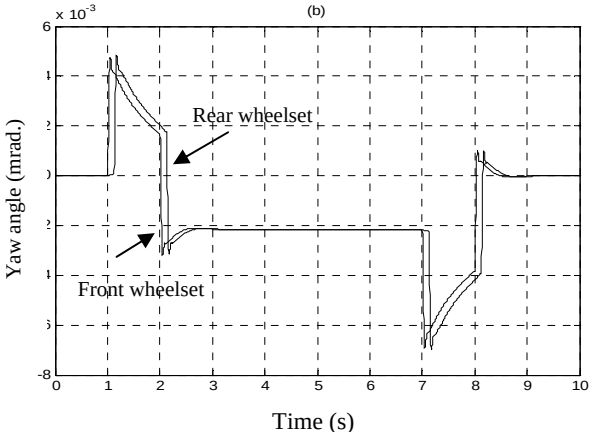

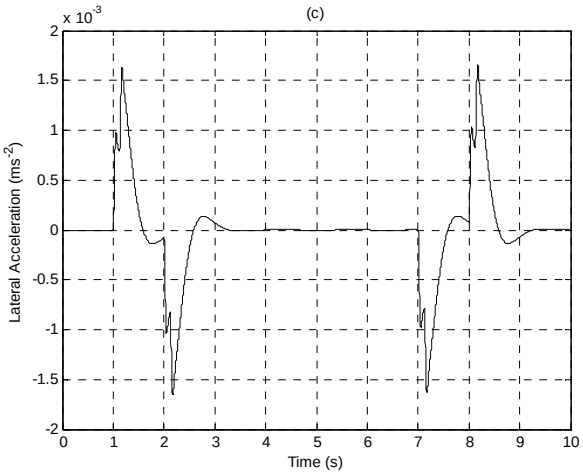

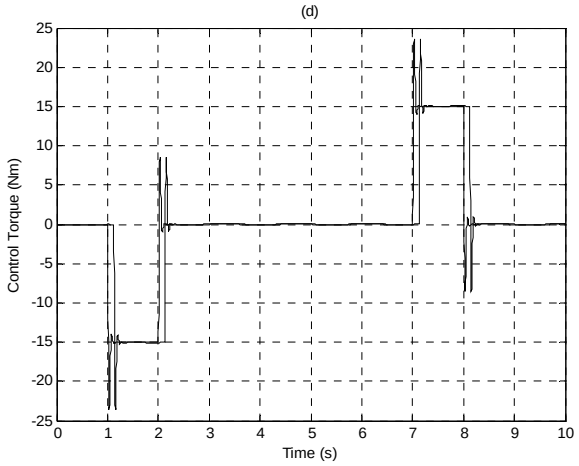

Figure 8. Two-axle vehicle with IRW

5. CONCLUSIONS

From the findings presented in this paper, it can be concluded that the two-axle vehicle performs better during curving than the bogie-based vehicle especially when minimum wheelset lateral displacement (for reduced wear and tear of the wheelset) and control effort are of our main concern. It also has the advantage of lighter and simpler configuration. It can also be concluded that the IRW provide better curving performance than solid-axle wheelset, although with this type of wheelset natural curving capability of the conical/profiled wheelset is eliminated.

ACKNOWLEDGEMENT

The authors would like to thank Universiti Teknologi Malaysia and Universiti Malaysia Pahang for their supports.

REFERENCES

[1] A.H. Wickens, "The dynamics of railway vehicles – from Stephenson to Carter," *Proc. Instn. Mech. Engnrs. Part F*. vol. 212, pp. 209-217, 1998.

[2] W.H. Elmaraghy, "Ride quality and dynamics of rail vehicle models for microcomputers," *Vehicle System Dynamics*, vol. 16, pp. 193-211, 1987.

[3] R.M. Goodall, "Tilting trains and beyond: The future for active railway suspensions (Part 2)," *Computing & Control Engineering Journal*, pp. 221 - 230, Oct. 1999.

[4] R.V. Dukkipati, S. Narayanaswamy, and M.O.M. Osman, "Independently-rotating wheelset systems for railway vehicles-a state of the art review," *Vehicle System Dynamics*, vol. 21, pp. 297-330, 1992.

[5] R.V. Dukkipati, and S. Narayanaswamy, "Performance of a rail car equipped with independently-rotating wheelsets having yaw control," *Jnl. of Rail and Rapid Transit*, vol. 213(1), pp. 31-38, 1999.

[6] R.M. Goodall, and H. Li, "Mechatronic developments for railway vehicles of the future,"

Proc. 1st IFAC Conference on Mechatronic Systems. Darmstadt, Germany, vol. 1, pp. 21-32, 2000.

[7] T.X. Mei, and R.M. Goodall, "Optimal control strategies for active steering of railway vehicle" *Proc. IFAC 1999*. Beijing, China, pp. 215-256, 1999

[8] Rail Safety & Standards Board. *Track System Requirement: Track Gauge*, London, April 2007.

[9] R.M. Goodall, "Tilting trains and beyond: The future for active railway suspensions (Part 1)," *Computing & Control Engineering Journal*, pp. 154, Aug. 1999.

APPENDIX

The system matrix (A) components for two-axle vehicle are shown below:

$a_{1,1} = a_{5,5} = -(2f_{22}/mV) - C_w/m$;

$a_{1,2} = a_{5,6} = -K_w/m$; $a_{1,4} = a_{5,8} = 2f_{22}/m$;

$a_{1,9} = a_{5,9} = C_w/m$; $a_{1,10} = a_{5,10} = K_w/m$;

$a_{1,11} = -a_{5,11} = C_w I_b/m$; $a_{1,12} = -a_{5,12} = K_w I_b/m$;

$a_{3,2} = a_{7,6} = -(2f_{11}l\lambda)/I_w r$;

$a_{3,3} = a_{7,7} = -(2f_{11}l^2)/I_w V$;

$a_{9,1} = a_{9,5} = C_w/m_v$; $a_{9,2} = a_{9,6} = K_w/m_v$;

$a_{9,9} = -2C_w/m_v$; $a_{9,10} = -2K_w/m_v$;

$a_{11,1} = -a_{11,5} = C_w l_b/I_v$; $a_{11,2} = -a_{11,6} = K_w l_b/I_v$;

$a_{11,11} = -2C_w l_b^2/I_v$; $a_{11,12} = -2K_w l_b^2/I_v$

Parameter used for two-axle vehicle with solid-axle wheelset and IRW:
V = vehicle speed (60 ms^{-1});
l = half gauge of wheelset (0.7 m);
r = wheel radius (0.45 m);
λ = conicity (0.2);
f_{11} = longitudinal creep coefficient (10 MN);
f_{22} = lateral creep coefficient (10 MN);
m = wheelset mass (1250 kg);
m_v = vehicle body mass (13500 kg);
I_w= wheelset yaw inertia (700 kgm^2);
I_v = vehicle body yaw inertia (170000 kgm^2);
I_{rw} = wheel yaw inertia (100 kgm^2);
l_b = half spacing between two wheelset (3.7 m);
R = curve radius (1500 m);
θ_c = cant angle (14^o);
g = gravity (9.81 ms^{-2});
K_w = lateral stiffness per wheelset (230 kN/m);
C_w = lateral damping per wheelset (50k Ns/m);

Parameter used for bogie-based vehicle:
V = vehicle speed (60 ms^{-1});
l = half gauge of wheelset (0.7 m);
r = wheel radius (0.45 m);
λ = conicity (0.2);
f_{11} = longitudinal creep coefficient (10 MN);
f_{22} = lateral creep coefficient (10 MN);
m = wheelset mass (1800 kg);
m_b = bogie mass (4000 kg);
m_v = vehicle body mass (45920 kg);
I_w = wheelset yaw inertia (1480 kgm^2);
I_b = bogie yaw inertia (5000 kgm^2);
I_v = vehicle body yaw inertia (2500000 kgm^2);
l_b = half spacing between two wheelsets (1.5 m);
l_v = half spacing between two bogies (8.5 m);
R = curve radius (1500 m);
θ_c = cant angle (14^o);
g = gravity (9.81 ms^{-2});
K_w = primary lateral stiffness per wheelset ($4x10^4$ kN/m);
C_w = primary lateral damping per wheelset (1200 kNs/m);
K_s = secondary lateral stiffness per wheelset (1900 kN/m);
C_s = secondary lateral damping per wheelset (60 kNs/m);